

Journal of Materials Chemistry A

Accepted Manuscript



This is an *Accepted Manuscript*, which has been through the Royal Society of Chemistry peer review process and has been accepted for publication.

Accepted Manuscripts are published online shortly after acceptance, before technical editing, formatting and proof reading. Using this free service, authors can make their results available to the community, in citable form, before we publish the edited article. We will replace this *Accepted Manuscript* with the edited and formatted *Advance Article* as soon as it is available.

You can find more information about *Accepted Manuscripts* in the [Information for Authors](#).

Please note that technical editing may introduce minor changes to the text and/or graphics, which may alter content. The journal's standard [Terms & Conditions](#) and the [Ethical guidelines](#) still apply. In no event shall the Royal Society of Chemistry be held responsible for any errors or omissions in this *Accepted Manuscript* or any consequences arising from the use of any information it contains.

Doping Activated Carbon Incorporated Composite MIL-101 using Lithium: Impact on Hydrogen Uptake

Prasanth Karikkethu Prabhakaran, Johnny Deschamps*

Unité Chimie et Procédés (UCP), École Nationale Supérieure de Techniques Avancées (ENSTA ParisTech), Université PARIS-SACLAY, 828 Boulevard des Maréchaux, 91762 Palaiseau Cedex, France.

*Email: johnny.deschamps@ensta-paristech.fr, Tel.: +33 1 81 87 20 11

ABSTRACT

Metal-organic frameworks (MOFs) have attracted considerable attention in the past several years in the area of hydrogen storage. Various modification strategies have been performed to enhance the hydrogen storage capacity in MOFs both at room temperature and cryogenic temperatures. In this study a hybrid composite MOF was synthesised by adding activated carbon (AC) NORIT-RB3 *in situ* during the synthesis of MIL-101 and lithium doping at various lithium ion concentrations were done in the synthesised composite material. Hydrogen adsorption-desorption studies were performed at 77 K and 298 K up to 100 bar in all the samples. For all materials studied, isosteric heat of adsorption has been calculated from the measured isotherms of adsorption. The results of adsorption showed that the hydrogen uptake capacity of MIL-101 could be considerably enhanced by the combined modification of MIL-101 using activated carbon and lithium doping. Here we present a simple way which can enhance the hydrogen uptake capacity of MIL-101 material at 77 K and 298 K. Activated carbon NORIT-RB3 is not costly compared to other carbon materials such as carbon nanotubes and thus this method is very cheap also. However the percentage of lithium doping should be controlled since large concentrations of lithium destroy the framework structure of MIL-101.

KEY WORDS

Hydrogen adsorption, Lithium doping, Metal-Organic Framework (MOF), MIL-101, Activated carbon, Composite MOF.

1. INTRODUCTION

Hydrogen storage is the key technology to be addressed before using hydrogen as an energy carrier for onboard vehicular applications.¹ Various materials like zeolites,^{2, 3} mesoporous silica materials,³ carbonaceous materials⁴ etc have been studied till date for hydrogen storage applications but none of them achieved the DOE target for practical hydrogen storage at ambient conditions.⁵ The DOE target for a sustainable hydrogen economy involves developing materials which can store up to 5.5 weight percent of hydrogen by 2017. Basically two methods were used for hydrogen storage, the chemical storage (chemisorption) of hydrogen and physical storage (physisorption). In chemisorption hydrogen binds via strong chemical bonds such as in complex hydrides and metal hydrides and in physisorption hydrogen binds to the surfaces of porous adsorbents by very weak dispersion interactions.⁶ In comparison with chemisorption, physisorption of hydrogen in porous materials has attracted more attention due to its fast kinetics and complete reversibility.

Metal-organic frameworks are new class of crystalline materials composed of inorganic sub units and rigid organic linkers with extremely high surface area values and porosity.⁷⁻¹³ The porous framework structure in MOFs makes them useful as adsorbents for various gases such as hydrogen, carbon dioxide and methane. MOFs have infinite variety of possible framework structures with tunable and well defined pores, high surface areas and pores volumes. These unique properties of MOFs made them useful in a variety of applications such as gas storage,¹⁰ gas separation,¹¹ adsorption, catalysis and sensors.^{12, 13} Since MOFs possesses very large surface area values and tunable pores, makes them an attractive class of materials to meet these goals and there have been various reports of hydrogen storage in MOF materials.

Different strategies for enhancing the H₂-surface interaction have been explored,¹⁴ including systematically varying pore structure,¹⁵ minimizing pore size to increase van der Waals contacts with hydrogen,¹⁶ and embedding coordinatively unsaturated metal centers within the MOF structure to interact better with H₂.¹⁷ An alternative approach for strong H₂ binding comes from the possibility of doping light alkali metal cations such as Li⁺, Na⁺, Mg²⁺ into the porous framework of MOFs and thereby increasing the binding energy for hydrogen adsorption.^{18, 19} Among this lithium ion is more promising due to its low atomic weight and high affinity towards hydrogen by charge induced dipole interactions.¹⁹ Theoretical studies in alkali metal doped fullerenes have shown higher hydrogen adsorption capacity and theoretical calculations in lithium coated fullerenes impregnated inside lithium doped IRMOF-10 showed

hydrogen storage capacity of 6.3 wt% at 100 bar and 243 K.^{20, 21} Klontzas et al. by simulation studies showed an improved hydrogen storage capacity in MOFs by functionalization of organic linker with lithium atoms.²² Simulation studies have shown that doped Li ions in MOF donates ~0.9 electron to the MOF linker and results in a H₂ binding energy of about 12 kJ mol⁻¹ and strong binding to Li near MOF corners.^{23, 24} Ghoufi, Deschamps and Maurin reported a substantial increase in hydrogen storage capacities up to 10 wt% in Li modified MIL-101 at 77 K by grand canonical monte carlo (GCMC) simulations.²⁵ Simulation studies by Meng et al. in lithium doped IRMOF-9 have shown hydrogen storage capacity of 4.04 wt% at 298 K and 100 bar.²⁶ Theoretical studies have also shown that lithium doped MOFs and COFs can store more than 6 wt% of hydrogen at ambient conditions.^{27, 28} Experimental studies by Li et al. have shown hydrogen storage capacity of 6.1 wt% at 1 bar and 77 K in lithium doped conjugated microporous polymers.²⁹ There was also experimental reports that lithium doped MOFs have shown increased uptake capacity at 77 K.³⁰⁻³⁴ Researchers have shown increase in low pressure hydrogen uptake capacity by lithium doping using a post synthetic alkoxide formation in MOFs containing peculiar functional groups.^{33, 34} But this modification method can only be applied to a few MOFs having peculiar functional groups in their framework, therefore a new lithium doping method should be developed which can be applied in variety of other MOFs. Another approach for increasing hydrogen uptake capacities in MOFs are by doping with carbon nanotubes and activated carbon.^{35, 36} Doping of these carbonaceous materials in MOFs have given them an enhanced composite performance with unusual mechanical and hydrophobic properties.³⁷ Moreover these hybrid composite MOFs have more thermal stabilities and better moisture resistance compared to bare MOFs. Based on these observations in our present study we have synthesised a hybrid composite MOF by incorporating activated carbon into the porous framework of MIL-101 *in situ* during the synthesis and performed lithium doping in this composite MIL-101 using lithium naphthalenide (C₁₀H₇Li) to get the synergic effect of both activated carbon incorporation and lithium doping. MIL-101 was chosen for this study to obtain a fine dispersion of the doped activated carbon and lithium insides the pores of MOF as it possesses very high surface area values, pore volume and thermal stabilities compared to other MOFs. MIL-101 is a chromium (III) terephthalate MOF material first reported by Ferey et al.³⁸ with a mesoporous zeotype architecture assembled by corner-sharing super tetrahedra, which consist of Cr₃O trimers and 1, 4-benzenedicarboxylic acids. It contains numerous unsaturated Cr metal sites, and two types of mesoporous cages (29 and 34 Å in diameter) with microporous windows (12 and 16 Å in diameter).³⁹ This material has a giant cell volume, a very high surface area, large pores

and high thermal and chemical stabilities which makes it an important candidate for diverse applications such as gas adsorption, separation and catalysis.⁴⁰ Activated carbon NORIT- RB3 is very much cheaper and easily available compared with carbon nanotubes (price 5700 times lower according to Sigma Aldrich) which were used as dopants for MOFs in previous studies.^{35,37}

2. EXPERIMENTAL DETAILS

2.1. Materials and methods

Chromium (III) nitrate ($\text{Cr}(\text{NO}_3)_3 \cdot 9\text{H}_2\text{O}$), 1,4-benzenedicarboxylic acid (H_2BDC), acetic acid ($\text{C}_2\text{H}_4\text{O}_2$), nitric acid (HNO_3), hydrogen peroxide (H_2O_2), ammonium fluoride (NH_4F), naphthalene (C_{10}H_8) were supplied by Sigma-Aldrich and were used as received. Tetrahydrofuran (THF) purified by the solvent purification system (MBRAUN) was used for synthesis. Lithium wire (Aldrich) was immersed in THF to remove excess mineral oil and the surface oxide coating to get the metallic surface. All the preparation procedures for lithium naphthalenide ($\text{C}_{10}\text{H}_7\text{Li}$) and lithium doping were performed under argon atmosphere in a glove box.

2.2. Preparation of activated carbon (AC) incorporated MIL-101 (AC-MIL-101) and Li Doping

The NORIT-RB3 activated carbon (AC) obtained from Sigma Aldrich was treated with $\text{HNO}_3/\text{H}_2\text{O}$ (1:1 v/v) for purification and functionalization. The functionalized AC (25 mg) was mixed with 60 mL of H_2O containing 4.0 g of chromium (III) nitrate nonahydrate ($\text{Cr}(\text{NO}_3)_3 \cdot 9\text{H}_2\text{O}$), 1.66 g of 1,4-benzene dicarboxylic acid (H_2BDC), and 0.56 mL of acetic acid. The mixture was ultrasonicated during 10 minutes in a 75 mL Teflon lined stainless steel autoclave and the bomb was placed in a preheated oven at 493 K for 8 h. After the reaction the bomb was cool down to room temperature. The reaction mass was then double filtered first with glass frit of pore size 2 and then with pore size 5 to remove the residual H_2BDC present as white needle like crystals in the crude product. The filtered product was washed with hot water and dried at 353 K in an oven. The crude MIL-101 was then stirred in 30 mM NH_4F solution at 333 K for 12 h to remove unreacted H_2BDC trapped inside the pores. The precipitate was filtered under hot conditions and washed several times with 300 mL of hot water (333 K) to remove any traces of H_2BDC and NH_4F . The same procedure was used for the preparation of bare MIL-101 except the addition of activated carbon. AC-MIL-101 samples were activated under vacuum at 423 K for 12 h prior to lithium doping. Lithium naphthalenide ($\text{C}_{10}\text{H}_7\text{Li}$) solution was used for the doping of Li^+ ions into activated AC-MIL-101 frameworks. The solution was prepared by addition of an equimolar amount of clean

lithium into 0.05 M solution of naphthalene in dry THF under vigorous stirring. The solution was ultrasonicated for another 15 minutes for completing the reaction. The lithium naphthalenide solution was then calibrated by hydrochloric acid (HCl) of standard concentration until the pH is neutral. A precise quantity of the prepared lithium naphthalenide solution (corresponding to the concentration of lithium doping) was transferred by syringe into 30 mL THF with 200 mg of activated AC-MIL-101 sample in a round bottom flask. The mixture was vigorously stirred 12 h and then isolated by filtration and washed with THF and immersed in dry THF for one day to remove any traces of adsorbed naphthalene. The quantity of lithium naphthalenide was varied to get three different concentrations of lithium doped AC-MIL-101 samples.

2.3. Characterization

Powder X-ray diffraction (PXRD) measurements of MIL-101, AC-MIL-101 and lithium doped AC-MIL-101 samples were performed in a Bruker AXS D8 Advance system in the 2θ range 1.5° to 15° at a scan speed of $0.1^\circ \text{ sec}^{-1}$ using $\text{CuK}\alpha$ ($\lambda=1.54056 \text{ \AA}$) radiation to determine the framework crystallinity. The FTIR spectra of all the MIL-101 samples were done in a Bruker TENSOR 27 spectrometer with a special accessory for powdered samples in the wave number range of $4000\text{-}600 \text{ cm}^{-1}$. The thermal stabilities of MIL-101, AC-MIL-101 and Li@AC-MIL-101-B samples were investigated using Setaram LabSys evo TGA-DTA system starting from 303 K – 873 K at a heating rate of 10 K min^{-1} under argon flow of 20 mL min^{-1} . The concentration of lithium ions inside the lithium doped samples were measured using an atomic absorption spectrometer (Thermo Electron Corporation). Elemental analysis for the percentage of carbon inside MIL-101 was performed using CHN analyser (PerkinElmer- 2400). The percentage of BET surface area and pore volume of all the MIL-101 samples were determined in a static volumetric adsorption system (Micromeritics Tristar II 3020) using N_2 adsorption-desorption isotherm at 77 K up to 1 bar. Before adsorption measurements the samples were degassed by heating up to 423 K under vacuum for 8 h. The BET surface area was obtained with the Brunauer–Emmett–Teller (BET) treatment of the isotherms in the p/p_0 range of $0.05 - 0.25$. The nonlocal density functional theory (NLDFT) method was used to calculate the pore size distribution (PSD) curves in MIL-101 and composite samples from N_2 adsorption data measured at 77 K .

2.4. High Pressure Hydrogen Adsorption Measurements

Hydrogen adsorption isotherms at 77 K and 298 K up to 100 bar were measured using gravimetric sorption analyzer (Rubotherm IsoSORP[®] GmbH, Germany) equipped with a

magnetic suspension balance (MSB). There are two different operating positions for the MSB. In the first step when the measurement cell is filled with H₂ gas, MSB records the weight change of the sample that is placed in the sample container as the high pressure gas is adsorbed by the sample. The second measurement position is to measure the *in situ* density of the high pressure gas, which is necessary for the calculation of amount of H₂ gas adsorbed onto the sample in the cell. Pressure was measured with a two pressure transducers PIRC-1 and PIRC-2 depending of the pressure inside the system. In a pressure range higher than 34 bar the pressure transducer PIRC-1 is used and for pressures below 34 bar a more sensitive PIRC-2 is used to visualize the pressure inside the system. Hydrogen adsorption measurement at 77 K was performed by immersing the measuring cell in a liquid nitrogen bath equipped with an automatic level controller which constantly maintains the level of liquid nitrogen throughout the time of measurement. For ambient temperature hydrogen adsorption study the temperature of the measurement cell was maintained at 298 K throughout during the measurement using a Julabo CF-41 temperature controller. In a typical hydrogen adsorption measurement initially a blank measurement was performed with H₂ without the sample to measure the empty weight and volume of the sample cell. The MOF sample was then loaded to the sample cell and degassed at 423 K under vacuum over night to remove any pre-adsorbed gases and solvents. A buoyancy measurement was performed at 298 K using helium gas to measure the volume of MOF sample loaded for hydrogen adsorption.⁴¹ Hydrogen gas at elevated pressure was added incrementally and data points were recorded when the mass stability was reached.

2.5. Isosteric heat of adsorption

Isosteric heat of adsorption has been calculated from the available experimental data. This isosteric heat of adsorption was calculated from the adsorption isotherms measured at 77 K and 298 K using the Clausius-Clapeyron equation which relates the adsorption heat effects to the temperature dependence of the adsorption isotherm at a specific amount adsorbed. The equation used is expressed as follows:^{42, 43}

$$\Delta H = -R \left[\frac{\partial \ln(p)}{\partial (1/T)} \right]_n$$

Where R is the ideal gas constant, p the pressure, T the temperature and n the specific amount adsorbed. Two approximations are introduced in deriving the Clausius-Clapeyron equation: the bulk gas phase is considered ideal and the adsorbed phase volume is neglected. These two assumptions are reasonable at low pressures but may be not true at high pressures.⁴²

Considering this constraint and the weak hydrogen adsorption at 298 K, the calculations have been performed over a pressure (0-20 bar) range and a single specific amount of adsorbed gas which correspond to a weight fraction of 0.15%. Additionally the calculations were performed using only two isotherms measured over a wide temperature (77-298 K) range and this leads to a consequent uncertainty. Nevertheless the results obtained provide an acceptable approximation of the isosteric heat of adsorption of the different systems which can be helpful to characterise the hydrogen adsorption properties of the materials and to explain the physical phenomena of the adsorption process.

3. RESULTS AND DISCUSSION

The PXRD patterns of MIL-101, AC-MIL-101 and lithium doped AC-MIL-101 samples (Figure 1) were in good agreement with published results in literature.³⁸ This indicates that the framework structure and crystallinity of MIL-101 was not affected by activated carbon incorporation and lithium doping.³⁶ The FTIR spectra of MIL-101, AC-MIL-101 and lithium doped AC-MIL-101 samples are shown in Figure 2. The infrared frequency vibrational band at 1635 cm^{-1} indicates the presence of adsorbed water and the strong band at 1397 cm^{-1} is due to the symmetric (O-C-O) vibrations dicarboxylate within the framework of MIL-101.⁴⁴ The other bands between 600 and 1600 cm^{-1} are due to benzene ring. The band at 1510 cm^{-1} is attributed to the (C=C) stretching vibration and bands at 1165, 1020, 880 and 743 cm^{-1} were attributed to the (C-H) deformation vibrations.

The thermal stabilities of MIL-101, AC-MIL-101 and one lithium doped AC-MIL-101 samples were studied by thermo gravimetric analysis (TGA). The TGA plots (Figure 3) obtained were well matched with the results published in literature and showed three distinct weight loss steps.^{36, 40} The first step from 303 K–473 K corresponds to the loss of guest water molecules from the large cages ($d = 34 \text{ \AA}$).^{38, 40} The second weight loss step from 473 K–623 K is due to the loss of water molecules from the middle sized cages ($d = 29 \text{ \AA}$).⁴⁵ The third weight loss step above 623 K is due to the elimination of –OH and other coordinated groups leading to the framework decomposition of MIL-101.³⁸ Results indicate that all samples showed remarkable thermal stability with a decomposition temperature higher than 623 K under argon atmosphere. The plots also showed that the thermal stability and hydrophobicity of MIL-101 increased after activated carbon incorporation.^{35, 36} Elemental analysis of AC-MIL-101 sample showed 2.6 wt%. of activated carbon was incorporated inside MIL-101 by doping.

The nitrogen adsorption-desorption isotherms of MIL-101, AC-MIL-101 and Li doped AC-MIL-101 samples are shown in Figure 4. The BET surface area of MIL-101 obtained is $3148 \text{ m}^2 \text{ g}^{-1}$, which was in good agreement with reported value.³⁸ The total pore volume of MIL-101 is estimated to be $2.19 \text{ cm}^3 \text{ g}^{-1}$ and the pore size distribution curve showed two domains of pore sizes at 25 and 30 Å which were also in accordance with the literature.³⁸ The BET surface area of MIL-101 was increased after activated carbon incorporation as reported earlier.³⁶ However after the lithium doping the surface area values and pore volume have shown a decreasing trend as the concentration of lithium increased inside the framework by doping as the doped Li ions occupies the pores of MIL-101 framework and leads to the reduction in surface area values. The NLDFT pore size distribution curves (Figure 5) also supports this findings. The NLDFT calculations take into consideration the configuration of adsorbed molecules in pores on a molecular level and allows to obtain a more accurate and comprehensive pore size analysis over complete micro/meso pore size range compared with macroscopic, thermodynamic methods, namely, BJH (Barret-Joyner-Halenda), HK (Horvath-Kawazoe), SF (Saito-Foley), and DR (Dubinin-Radushkevich).⁴⁶ Conventional techniques such as macroscopic or thermodynamic methods (e.g. BJH which works on Kelvin equation) assume bulk fluid-like behaviour for pore fluid and neglect details of the fluid-wall interactions. The concentration of lithium, BET surface area, pore volume and hydrogen uptake capacities of the lithium doped and pristine samples are given in Table 1. The doped lithium is presumably in the ionic state and the lithium cations are coordinated with the carboxyl groups as reported in the case of Li doped MIL-53(Al) by Kubo et al. using solid state NMR studies.³² The maximum lithium concentration tested was 1078 ppm in Li@AC-MIL-101-C sample and the BET surface area of this sample was largely reduced due to the excessive lithium ion concentration since at high lithium concentration, Li^+ ions substitute the Cr^{3+} sites which destroys the framework structure of MIL-101.³³

Hydrogen adsorption studies were performed in MIL-101, AC-MIL-101, Li@MIL-101 and Li@AC-MIL-101 samples at 77 K and 298 K up to 100 bar pressure. The high pressure hydrogen adsorption-desorption isotherms measured at 77 K and 298 K are shown in Figure 6 and Figure 7 respectively. The lithium doped MIL-101 sample showed higher hydrogen sorption capacity compared to bare MIL-101.³⁰⁻³⁴ Mulfort et al. have reported that lithium doped MOF showed nearly double hydrogen storage capacity of 1.63 wt% compared to 0.93 wt% in undoped MOF at 77 K and 1 bar pressure.³⁰ In the same conditions of temperature and pressure (77 K under 1 bar), the hydrogen storage capacity between the undoped MIL-

101 and the Li@AC-MIL-101-B materials shows a quite similar behaviour: the Li@AC-MIL-101-B sample showed a hydrogen uptake of 1.60 wt% compared to 1.20 wt% in undoped MIL-101. The hydrogen uptake capacities of AC-MIL-101 samples at 77 K and 298 K up to 100 bar pressure were also considerably enhanced by lithium doping. But further doping of lithium decreased the hydrogen uptake capacity as excessive doping of lithium destroy the structure of MIL-101 as evidenced by PXRD and BET surface area measurements. This clearly shows a controlled doping of lithium is necessary to obtain a positive result. The sample Li@AC-MIL-101-B with 727 ppm concentration of lithium showed the maximum H₂ uptake capacity of 143.9 and 11.4 mg g⁻¹ at 77 K and 298 K respectively up to 100 bar pressure, which is almost double the hydrogen uptake capacity of MIL-101 at the same conditions. The hydrogen uptake capacities obtained for MIL-101 at 77 K and 298 K at 100 bar was 72.5 and 5.50 mg g⁻¹ which were comparable with the reported literature datas of 61.0 and 4.30 mg g⁻¹ at 77 K and 298 K up to 80 bar respectively as reported by Latroche et al.⁴⁷ Almost all the reported experimental works on hydrogen adsorption in lithium doped MOFs were at low pressure up to 1 bar only, as per our knowledge experimental reports on high pressure hydrogen adsorption studies in lithium doped MOFs were not found in literature. Theoretical studies by Han et al. have predicted gravimetric hydrogen uptake capacity of 51.6 mg g⁻¹ (5.16 wt%) in lithium doped MOF-C30 at 300 K and 100 bar.²⁷ Simulation studies by Cao et al. have suggested doping with lithium in COF-108 and COF-105 enhanced their gravimetric hydrogen uptake capacity to reach 68.4 and 67.3 mg g⁻¹ (6.84 and 6.73 wt%) respectively at 298 K and 100 bar pressure.²⁸ Eventhough the maximum hydrogen uptake capacity obtained at 298 K and 100 bar for Li@AC-MIL-101-B sample was much lesser compared with the results reported by simulation studies, the method of lithium doping in AC-MIL-101 is promising to develop new porous materials for hydrogen storage applications.

The isosteric heats of adsorption calculated from available experimental data (adsorption isotherms measured at 77 and 298 K) for all materials studied are listed in the Table 2. As explained in the section 2.5 these calculations are associated to a consequent uncertainty and can be considered as an approximation only. Nevertheless, the value calculated of 4.3 kJ.mol⁻¹ for the MIL-101 material is in very good agreement with the result of 4.3 kJ.mol⁻¹ obtained from Shmitz et al.⁴⁸ According to the Figures 6 and 7 lithium doping in bare MIL-101 sample increases the hydrogen uptake and increases also the isosteric heat of adsorption. This result was in agreement with the conclusions of Mulfort et al.³³ concerning the lithium doping of the DO-MOF. The activated carbon (AC) doping of MIL-101 increases the hydrogen uptake and

slightly decreases the isosteric heat of adsorption. Finally the lithium doping of activated carbon incorporated composite MIL-101 decrease the isosteric heat of adsorption. This low value leads to a small hydrogen uptake at low pressure and a higher temperature dependence of the maximum hydrogen uptake.⁴⁸ These two remarks are in agreement with the adsorption measurements represented Figures 6 and 7. MIL-101 contains very large pores which have a diameter of 29 and 34 Å and it is not sure yet if adsorption take place in such huge pores or rather in smaller void of the material.⁴⁷⁻⁴⁹ Considering this physical property of MIL-101 it is difficult to correlate the isosteric heat of adsorption to the pore size of our materials.

At 77 K the adsorption-desorption isotherms are completely reversible whereas the desorption isotherms show a hysteresis at 298 K. According to the Figures 6 and 7, this hysteresis is probably due to the difference of kinetic of desorption at the two temperatures. To deeply understand this phenomenon, further studies are needed. Finally the doping of a little amount of lithium (727 ppm) in activated carbon incorporated MIL-101 almost doubled its hydrogen uptake capacity both at 77 K and 298 K up to 100 bar pressure. In MIL-101 the open metal sites which are responsible for hydrogen uptake were poisoned by the presence of unreacted benzene dicarboxylic acid (H₂BDC) moieties present inside the pores. The *in situ* activated carbon doping during synthesis may prevent the coordination of unreacted H₂BDC with the chromium metal sites and thus it is better available for interaction with hydrogen. The formation of ultramicropores inside MIL-101 by activated carbon incorporation also contributes towards the hydrogen uptake enhancement in AC-MIL-101 both at 77 K and 298 K.^{35, 36} Moreover studies have shown that lithium doping considerably increases the hydrogen uptake capacity in MOFs due to the strong affinity of lithium towards hydrogen molecule.¹⁸⁻²⁸ Hence the enhanced hydrogen uptake in lithium doped AC-MIL-101 sample in the present study may be attributed to the combined effect of these three factors, that is the formation of ultramicropores by activated carbon incorporation, activation of unsaturated metal sites by carbon incorporation and by the strong interaction of doped Li inside the pores of MIL-101 towards hydrogen.

4. CONCLUSIONS

The modification of MIL-101 both by activated carbon incorporation and lithium doping considerably enhanced the hydrogen uptake capacity of MIL-101. The doping of activated carbon incorporated MIL-101 with a little amount of lithium (727 ppm) almost doubled the hydrogen uptake capacity of the material both at 77 K and 298 K up to 100 bar. However excessive lithium doping leads to loss of crystallinity and framework decomposition, and

hence decrease in hydrogen uptake capacity. That means controlled doping of lithium and activated carbon is needed to get good surface area values and better interaction of hydrogen with the finely dispersed lithium inside the pores of MIL-101, which greatly enhanced the hydrogen uptake capacity. The combined modification of comparatively cheaper activated carbon incorporation and lithium doping and subsequent formation of a new hybrid composite MOF has provided a new and economically viable strategy for hydrogen sorption enhancement in MOFs.

ACKNOWLEDGEMENTS

The authors acknowledge the “Delegation Générale de l’Armement (DGA)” for financial support and Dr Elise Provost for her help concerning the characterizations by Atomic Absorption Spectrometry.

REFERENCES

- 1 L. Schlapbach and A. Züttel, *Nature*, 2001, **414**, 353–358.
- 2 K. P. Prasanth, R. S. Pillai, H. C. Bajaj, R. V. Jasra, H. D. Chung, T. H. Kim and S. D. Song, *Int. J. Hydrogen Energy*, 2008, **33**, 735-745.
- 3 K. P. Prasanth, H. C. Bajaj, H. D. Chung, K. Y. Choo, T. H. Kim and R. V. Jasra, *Int. J. Hydrogen Energy*, 2009, **34**, 888-896.
- 4 K. P. Prasanth, M. C. Raj, H. C. Bajaj, T. H. Kim and R. V. Jasra, *Int. J. Hydrogen Energy*, 2010, **35**, 2351-2360.
- 5 Targets for Onboard Hydrogen Storage Systems for Light Duty Vehicles, US DOE, 2009.
- 6 Y. Xia, Z. Yang and Y. Zhu, *J. Mater. Chem. A*, 2013, **1**, 9365-9381.
- 7 J. L. C. Rowsell and O. M. Yaghi, *Micropor. Mesopor. Mat.*, 2004, **73**, 3-14.
- 8 H. C. Zhou, J. R. Long and O. M. Yaghi, *Chem. Rev.*, 2012, **112**, 673-674.
- 9 N. Stock and S. Biswas, *Chem. Rev.*, 2012, **112**, 933-969.
- 10 M. P. Suh, H. J. Park, T. K. Prasad and D. W. Lim, *Chem. Rev.*, 2012, **112**, 782-835.
- 11 J. R. Li, J. Sculley and H. C. Zhou, *Chem. Rev.*, 2012, **112**, 869-932.
- 12 M. Yoon, R. Srirambalaji and K. Kim, *Chem. Rev.*, 2012, **112**, 1196-1237.
- 13 L. E. Kreno, K. Leong, O. K. Farha, M. Allendorf, R. P. Van Duyne and J. T. Hupp, *Chem. Rev.*, 2012, **112**, 1105-1125.
- 14 J. L. C. Rowsell and O. M. Yaghi, *Angew. Chem., Int. Ed.*, 2005, **44**, 4670-4679.
- 15 N. L. Rosi, J. Eckert, M. Eddaoudi, D. T. Vodak, J. Kim, M. O’Keefe and O. M. Yaghi, *Science*, 2003, **300**, 1127-1129.

- 16 D. J. Collins and H. C. Zhou, *J. Mater. Chem.*, 2007, **17**, 3154-3160.
- 17 M. Dinca and J. R. Long, *Angew Chem. Int. Ed.*, 2008, **47**, 6766-6779.
- 18 M. Barbatti, G. Jalbert and M. A. C. Nascimento, *J. Phys. Chem. A.*, 2002, **106**, 551-555.
- 19 R. C. Lochan and M. Head-Gordon, *Phys. Chem. Chem. Phys.*, 2006, **8**, 1357-1370.
- 20 K. R. S. Chandrakumar and S. K. Ghosh, *Nano Lett.*, 2008, **8**, 13-19.
- 21 D. Rao, R. Lu, C. Xiao, E. Kan and K. Deng, *Chem. Commun.*, 2011, **47**, 7698-7700.
- 22 E. Klontzas, A. Mavrandonakis, E. Tylianakis, G. E. Froudakis, *Nano Lett.*, 2008, **8**, 1572 – 1576
- 23 A. Blomqvist, C. M. Araujo, P. Srepusharawoot and R. Ahuja, *Proc. Natl. Acad. Sci. U.S.A.*, 2007, **104**, 20173-20176.
- 24 P. Dalach, H. Frost, R. Q. Snurr and D. E. Ellis, *J. Phys. Chem. C.*, 2008, **112**, 9278-9284.
- 25 A. Ghoufi, J. Deschamps and G. Maurin, *J. Phys. Chem. C.*, 2012, **116**, 10504-10509.
- 26 Z. Meng, R. Lu, D. Rao, E. Kan, C. Xiao and K. Deng, *Int. J. Hydrogen Energy*, 2013, **38**, 9811-9818.
- 27 S. S. Han and W. A. Goddard, *J. Am. Chem. Soc.*, 2007, **129**, 8422-8423.
- 28 D. P. Cao, J. H. Lan, W. C. Wang and B. Smit, *Angew. Chem., Int. Ed.*, 2009, **48**, 4730-4733.
- 29 A. Li, R. -F. Lu, Y. Wang, X. Wang, K. -L. Han and W. -Q. Deng, *Angew. Chem., Int. Ed.*, 2010, **49**, 3330-3333.
- 30 K. L. Mulfort and J. T. Hupp, *J. Am. Chem. Soc.*, 2007, **129**, 9604-9605.
- 31 K. L. Mulfort and J. T. Hupp, *Inorg. Chem.*, 2008, **47**, 7936-7938.
- 32 M. Kubo, A. Shimojima and T. Okubo, *J. Phys. Chem. C*, 2012, **116**, 10260-10265.
- 33 K. L. Mulfort, O. K. Farha, C. L. Stern, A. A. Sarjeant and J. T. Hupp, *J. Am. Chem. Soc.*, 2009, **131**, 3866-3868.
- 34 D. Himsl, D. Wallacher and M. Hartmann, *Angew. Chem., Int. Ed.*, 2009, **48**, 4639-4642.
- 35 K. P. Prasanth, P. Rallapalli, M. C. Raj, H. C. Bajaj and R. V. Jasra, *Int. J. Hydrogen Energy*, 2011, **36**, 7594-7601.
- 36 P. B. S. Rallapalli, M. C. Raj, D. V. Patil, K. P. Prasanth, R. S. Somani and H. C. Bajaj, *Int. J. Energy Research*, 2013, **37**, 746-753.
- 37 S. J. Yang, J. Y. Choi, H. K. Chae, J. H. Cho, K. S. Nahm and C. R. Park, *Chem. Mater.*, 2009, **21**, 1893-1897.

- 38 G. Férey, C. M. Draznieks, C. Serre, F. Millange, J. Dutour, S. Surble and I. Margiolaki, *Science*, 2005, **309**, 2040-2042.
- 39 O. I. Lebedev, F. Millange, C. Serre, G. V. Tendeloo and G. Férey, *Chem. Mater.*, 2005, **17**, 6525-6527.
- 40 D. Y. Hong, Y. K. Hwang, C. Serre, G. Férey and J. S. Chang, *Adv. Funct. Mater.*, 2009, **19**, 1537-1552.
- 41 K. Murata, K. Kaneko, F. Kokai, K. Takahashi, M. Yudasaka and S. Iijima, *Chem. Phys. Lett.*, 2000, **331**, 14-20.
- 42 H. Pan, J. A. Ritter and P. B. Balbuena, *Langmuir*, 1998, **14**, 6323-6327.
- 43 W. Zhou, H. Wu, M. R. Hartman and T. Yildirim, *J. Phys. Chem. C*, 2007, **111**, 16131-16137.
- 44 Q. Liu, L. Ning, S. Zheng, M. Tao, Y. Shi and Y. He, *Sci. Rep.* 2013, **2916 (3)**, 1-6.
- 45 S. H. Jung, J. H. Lee, J. W. Yoon, C. Serre, G. Férey and J. S. Chang, *Adv. Mater.* 2007, **19**, 121-124.
- 46 M. Thommes, Nanoporous Materials Science and Engineering; In Max Lu editors; Imperial College Press: London, 2004, 317-364.
- 47 M. Latroche, S. Surblé, C. Serre, C. M. Draznieks, P. L. Llewellyn, J. H. Lee, J. S. Chang, S. H. Jung and G. Férey, *Angew. Chem. Int. Ed.*, 2006, **45**, 8227-8231.
- 48 B. Schmitz, U. Müller, N. Trukhan, M. Schubert, G. Férey and M. Hirscher, *ChemPhysChem*, 2008, **9**, 2181-2184.
- 49 X. Lin, J. Jia, X. Zhao, K. M. Thomas, A. J. Blake, G. S. Walker, N. R. Champness, P. Hubberstey and M. Schroder, *Angew. Chem. Int. Ed.*, 2006, **45**, 7358-7364.

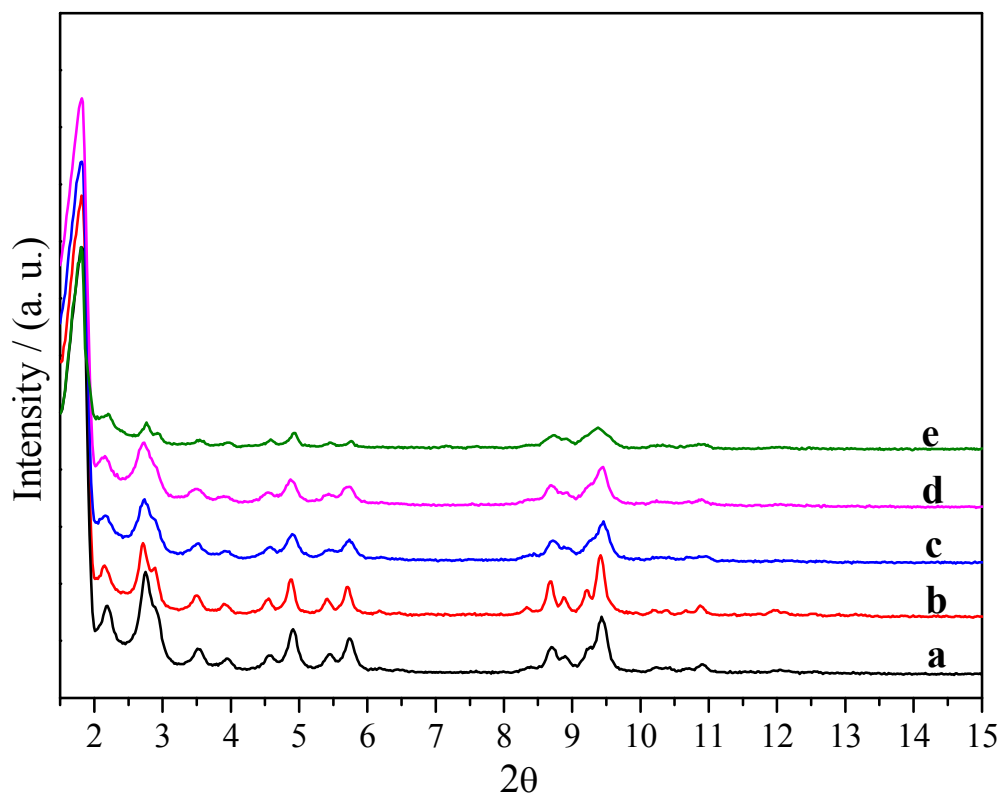


Fig. 1 PXRD patterns of (a) MIL-101, (b) AC-MIL-101, (c) Li@AC-MIL-101-A, (d) Li@AC-MIL-101-B and (e) Li@AC-MIL-101-C.

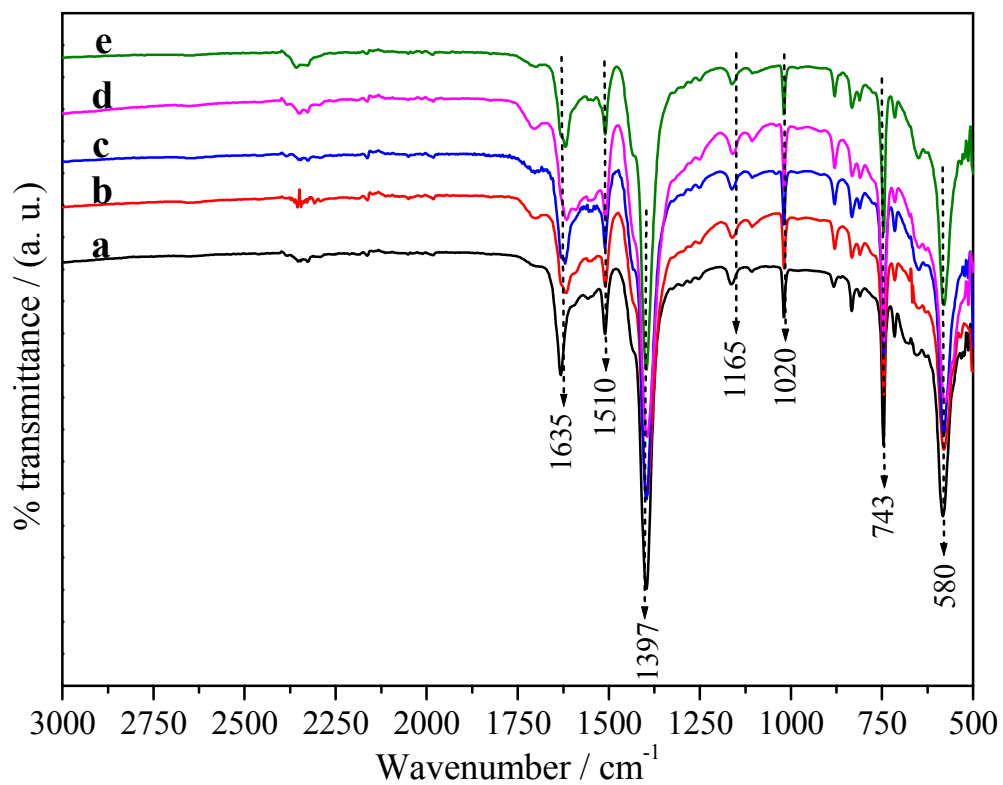


Fig. 2 FTIR spectra of (a) MIL-101, (b) AC-MIL-101, (c) Li@AC-MIL-101-A, (d) Li@AC-MIL-101-B and (e) Li@AC-MIL-101-C.

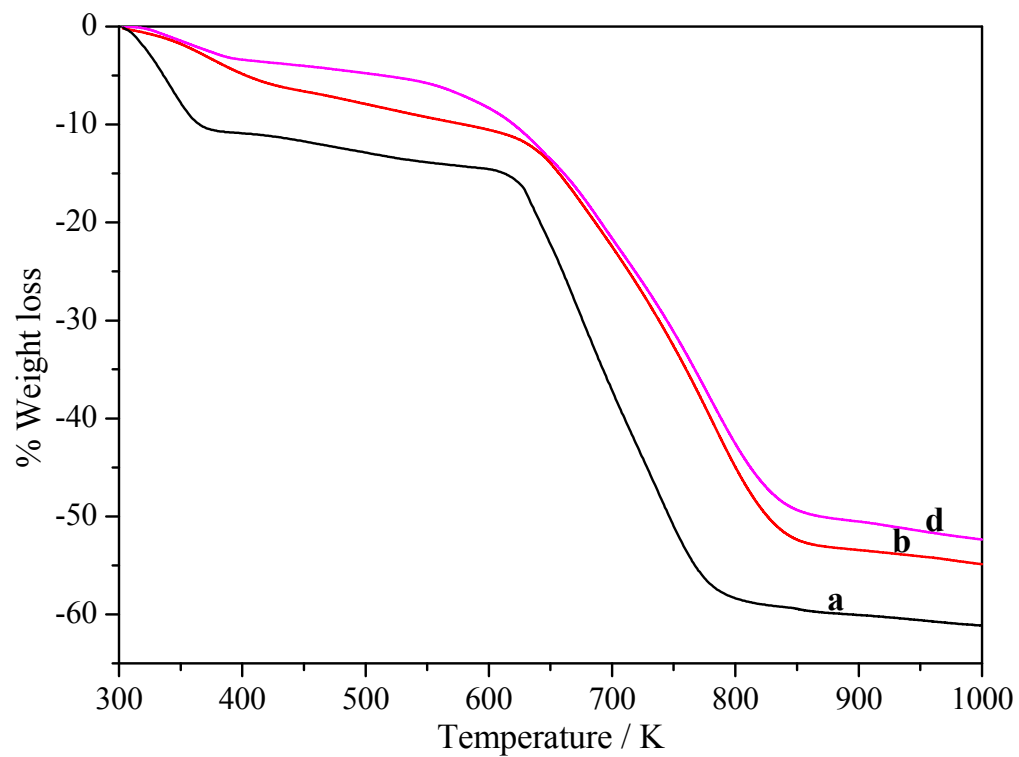


Fig. 3 TGA plots of (a) MIL-101, (b) AC-MIL-101 and (d) Li@AC-MIL-101-B.

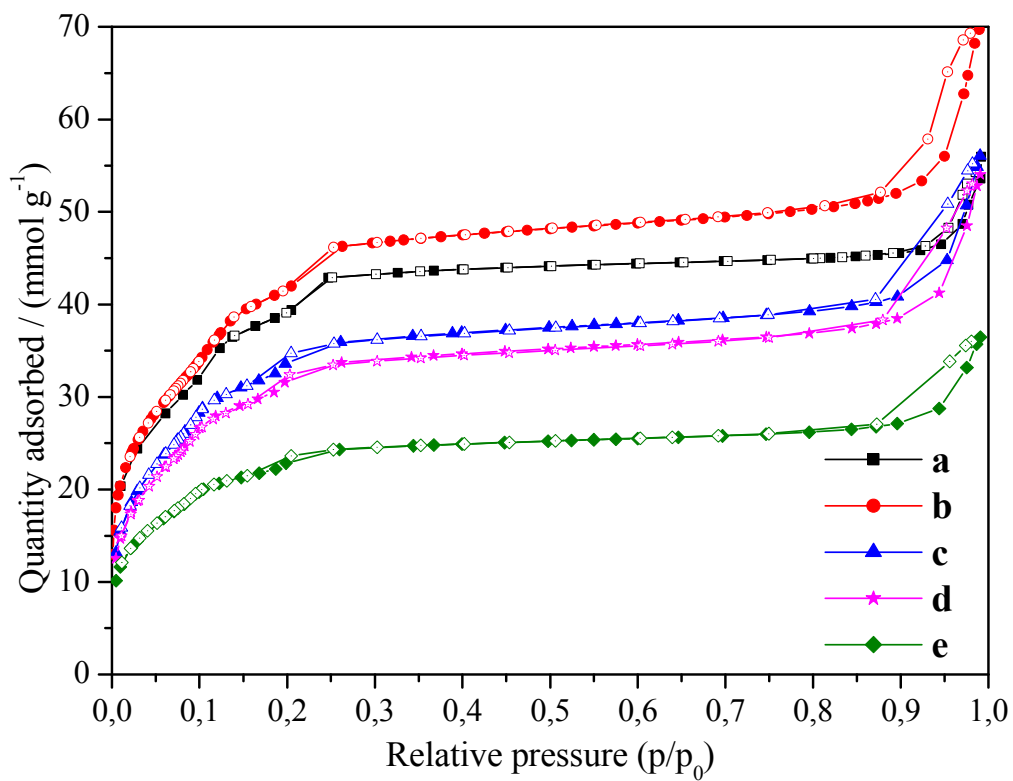


Fig. 4 N₂ adsorption-desorption isotherms of (a) MIL-101, (b) AC-MIL-101, (c) Li@AC-MIL-101-A, (d) Li@AC-MIL-101-B and (e) Li@AC-MIL-101-C.

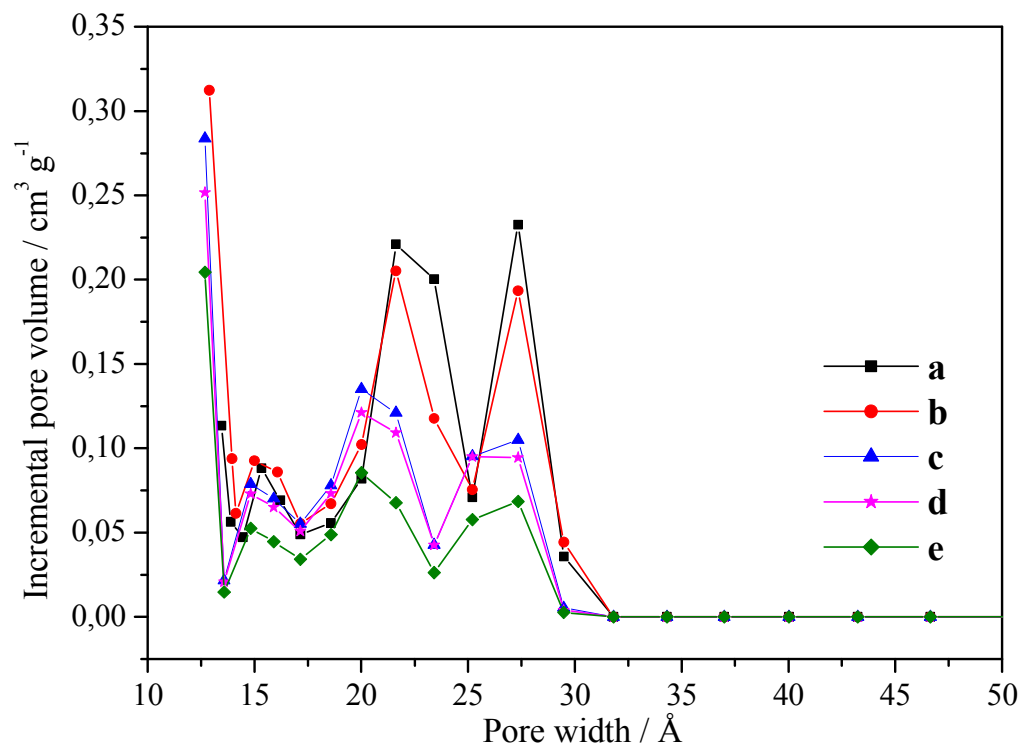


Fig. 5 NLDTF pore size distribution plots of (a) MIL-101, (b) AC-MIL-101, (c) Li@AC-MIL-101-A, (d) Li@AC-MIL-101-B and (e) Li@AC-MIL-101-C.

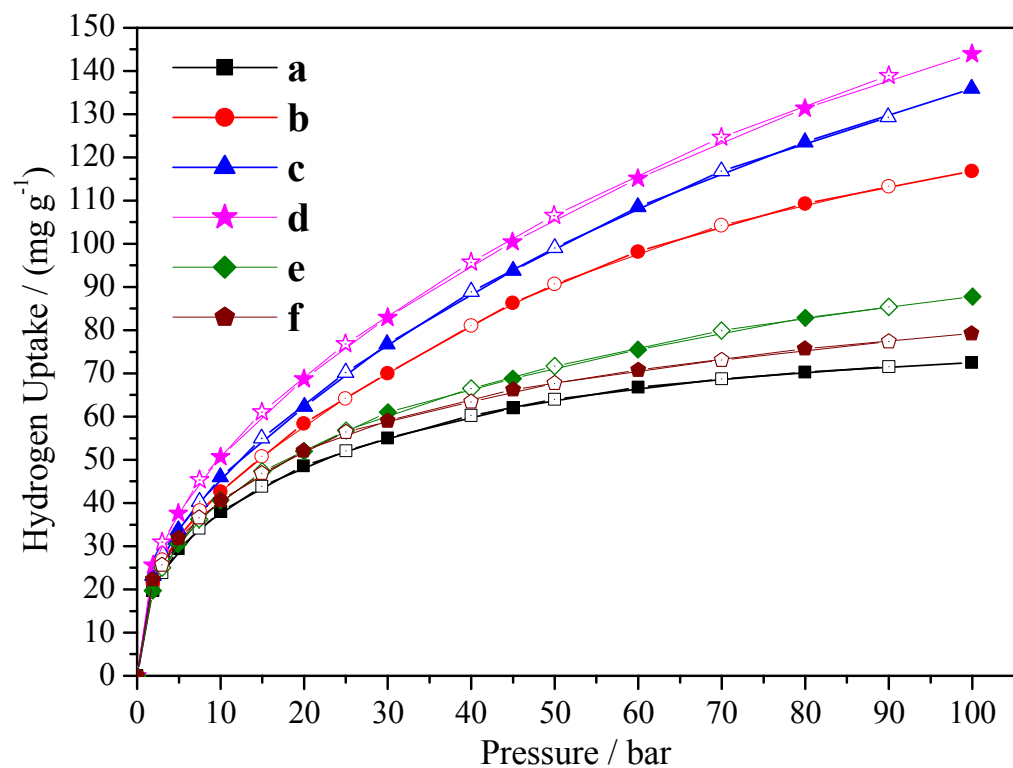


Fig. 6 High pressure hydrogen adsorption-desorption isotherms of (a) MIL-101, (b) AC-MIL-101, (c) Li@AC-MIL-101-A, (d) Li@AC-MIL-101-B, (e) Li@AC-MIL-101-C and (f) Li@MIL-101 at 77 K up to 100 bar. (Closed symbol = adsorption, open symbol = desorption).

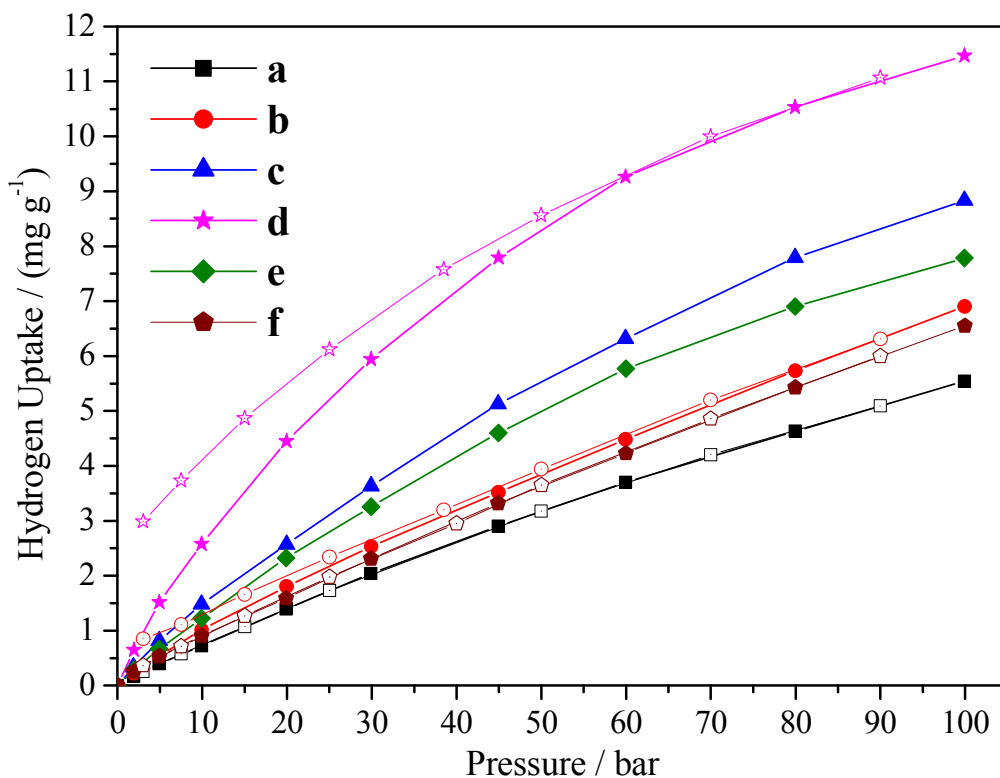


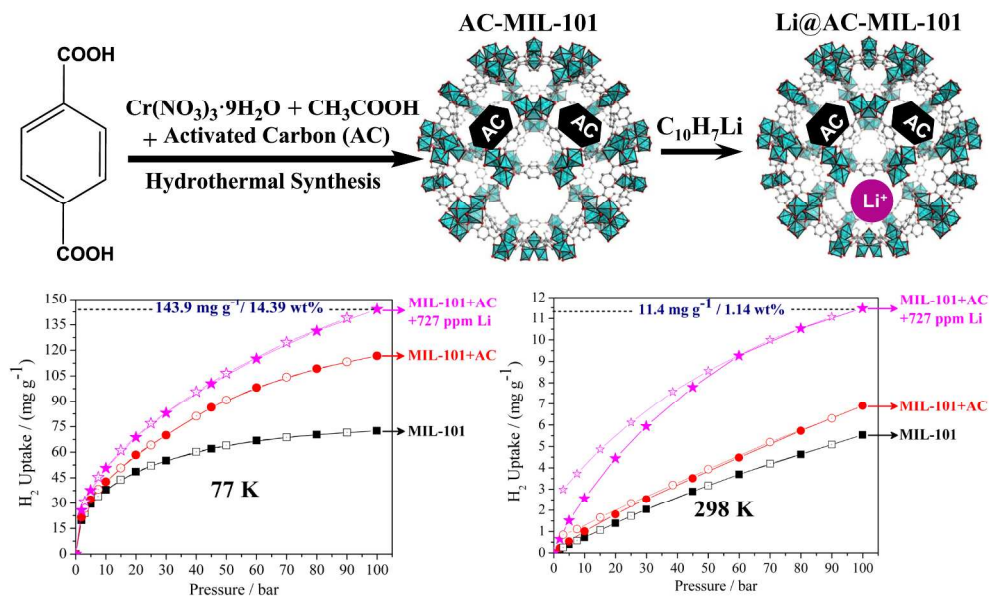
Fig. 7 High pressure hydrogen adsorption-desorption isotherms of (a) MIL-101, (b) AC-MIL-101, (c) Li@AC-MIL-101-A, (d) Li@AC-MIL-101-B, (e) Li@AC-MIL-101-C and (f) Li@MIL-101 at 298 K up to 100 bar. (Closed symbol = adsorption, open symbol = desorption).

Table 1. Lithium concentration and N₂ adsorption-desorption properties of MIL-101, AC-MIL-101 and Li doped AC-MIL-101 samples

Material	Concentration of Li (ppm)	BET Surface Area (m ² g ⁻¹)	Pore Volume (cm ³ g ⁻¹)	Hydrogen uptake capacity at 100 bar (mg g ⁻¹)	
				77 K	298 K
MIL-101	--	3148	2.10	72.50	5.50
AC-MIL-101	--	3458	2.04	116.8	6.90
Li@AC-MIL-101-A	394.0	2985	1.71	136.0	7.70
Li@AC-MIL-101-B	727.0	2791	1.65	143.9	11.4
Li@AC-MIL-101-C	1078	1868	1.09	87.70	8.80
Li@MIL-101	738.0	2383	1.44	79.20	6.55

Table 2. Isotheric heat of hydrogen adsorption calculated for the different samples synthesised.

Material	Isosteric heat of adsorption (kJ mol ⁻¹)	Isosteric heat of adsorption (kJ mol ⁻¹)
	(calculated values)	(literature values) ⁴⁸
MIL-101	4.3	4.3
AC-MIL-101	4.2	--
Li@AC-MIL-101-A	3.8	--
Li@AC-MIL-101-B	3.3	--
Li@AC-MIL-101-C	3.9	--
Li@MIL-101	4.4	--



254x152mm (300 x 300 DPI)